A strange novel chaotic system with fully golden proportion equilibria and its mobile microcomputer-based RNG application☆

Akin Ozdemir[a], Ihsan Pehlivan[b], Akif Akgul[c], Emre Guleryuz[d]

TUBITAK Informatics and Information Security Research Center
Kocaeli, Turkey

Department of Electrical and Electronics Engineering
Faculty of Technology, Sakarya University of Applied Sciences
54187, Sakarya, Turkey

[a]*akin.ozdemir3@ogr.sakarya.edu.tr, akin.ozdemir@tubitak.gov.tr*
[b]*ipehlivan@sakarya.edu.tr*
[c]*akifakgul@ieee.org, aakgul@sakarya.edu.tr*
[d]*emre.guleryuz1@ogr.sakarya.edu.tr*

Abstract

A strange novel three-dimensional quadratic continuous autonomous chaotic system with fully golden proportion equilibria is proposed. It has only seven terms, three quadratic nonlinearities and one parameter 'a'. The system equations have four equilibrium points and very interestingly all the equilibrium points have fully Golden Proportion values. Besides, this chaotic system has hidden amplitude control properties. The dynamic analyses of the system are presented such as equilibrium points, dissipativity, Lyapunov exponents, bifurcation diagrams, phase portraits and hidden amplitude control properties. Later, electronic circuit of the system is simulated in software and implemented in real environment. Finally, microcomputer-based random number generator (RNG) application and its NIST-800-22 tests are executed as another real-time application.

Keywords:
Chaotic systems, fully golden proportion, hidden amplitude control, electronic circuit realization, microcomputer-based RNG.

1. Introduction

After discovering and introducing first known chaotic system in the form of three-dimensional quadratic autonomous ordinary differential equations by Lorenz [1], lots of scientific researches have been carried out to discover new chaotic systems and attractors with different features [2, 3]. Especially during last decades more and more novel choatic systems have been found and introduced from different diciplines[4–8]. Detailed analyses and applications of several chaotic systems in different fields like physics, control, artificial neural networks, communications and computer science have been introduced in the literature [9–15].

Golden section [16] (golden proportion, golden mean) is another interesting interdisciplinary subject. There is presently an increasing interest of modern science in the applications of the golden section in many different fields such as several researches in crystallography [17], in astronomy, theoretical physics [18–22] and physics of the high energy particles [23–25]. Adapting a chaotic system to engineering applications often requires synchronization [26–28] and amplitude-phase control [29, 30]. There are also lots of different works related to chaos-based amplitude control in the literature [31–34].

It is really an interesting and challenging work to discover some nonlinear systems with fully golden proportion equilibria and hidden amplitude control properties like in this paper. Also, real time applications of these systems are exciting. In this paper, electronic circuit realizations and microcomputer based RNG design are executed for real-time applications. There are many works related to chaos-based applications with common chaotic systems in the literature [34–40].

Random numbers are used in lots of different applications such as computer games, lottery, chance games, Monte Carlo simulation and weather forecast [41, 42]. Random number generators are classified into 2 different groups as True-Random Number Generator (TRNG) and Pseudo-Random Number Generator (PRNG) depending on the producing method [43]. TRNG and PRNG can be implemented in software, hardware and hybrid structures. There are several entropy sources in literature to generate random numbers such as jitter [44], metastable [45], chaotic systems [46]. There are lots of chaos based RNG designs in the literature with different approaches; TRNGs based on mouse movement and chaotic cryptography [47], Piece-wise Affine Markov(PWAM) chaotic maps [48], chaos-modulated dual oscillator [49], performance metric for discrete-time chaos [50] and double scroll attractor.

Inspring from previous studies, in the intersection of chaos and golden section, a novel three dimensional continuous quadratic autonomous chaotic system with fully golden proportion equilibria is introduced in this article. In section 2, detailed analysis of fully golden proportion equilibria is presented and some common dynamical analysis such as phase portraits, dissipativity, equilibrium point analysis, lyapunov exponent spectrum and bifurcation diagram are investigated. In Section 3, hidden amplitude control properties of the system are investigated. In Section 4, a real electronic circuit design implementation of the proposed chaotic system is simulated in software and implemented in real environment. Furthermore, microcomputer-based RNG are designed and NIST-800-22 tests are applied. Finally, results are evaluated in conclusions.

2. A new 3D chaotic system with fully golden proportion equilibria and its dynamic analyses

The following strange chaotic system have fully golden proportion equilibrium points. The new chaotic system introduced in this paper is described as the following autonomous differential equations:

$$\begin{cases} \dot{x} = -x - yz, \\ \dot{y} = x - y - xz, \\ \dot{z} = xy + a, \end{cases} \tag{1}$$

Initial values of the new chaotic system are $x(0) = 1, y(0) = 0, z(0) = 0$. The system has only one constant parameter 'a'. In system (1) each equation contains a single quadratic cross-product term, and the linear terms in the first and second equations and a constant term in the third equation. Substituting a=1, the new system can be described by the following Eq. (2):

$$\begin{cases} \dot{x} = -x - yz, \\ \dot{y} = x - y - xz, \\ \dot{z} = xy + 1, \end{cases} \tag{2}$$

In this section, some dynamic behaviours of the chaotic system such as phase portraits, dissipativity, equilibrium points, lyapunov exponents spectrum and bifurcation are analyzed.

2.1. Phase portraits

To observe dynamic behaviors of the new systems,mathematical simulations are performed using Matlab ode45 function and phase portraits are obtained. $x - y, x - z, y - z$ plane (2D) phase portraits and $x - y - z$ plane (3D) are shown in Figure 1.

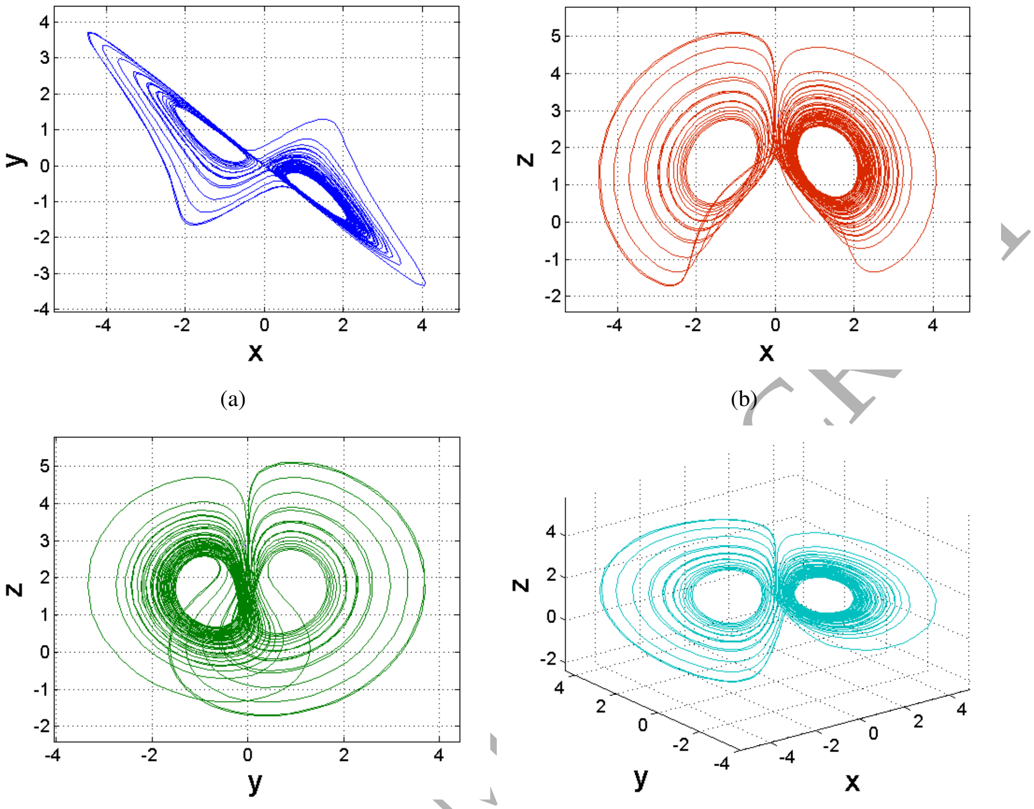

(a) (b) (c) (d)

Figure 1: Phase portraits of chaotic system (1) with parameter $a = 1$, a)$x - y$ plane, b)$x - z$ plane, c)$y - z$ plane, d)$x - y - z$ plane

2.2. *Dissipativity and equilibrium points analyses*

The new system has seven terms, three quadratic nonlinearities and one parameter 'a'. Typical parameter is a=1. Let us consider a volume in a certain domain of the state space. For the system (1), one has

$$\Delta \mathrm{V} = \frac{\partial \dot{\mathrm{x}}}{\partial \mathrm{x}} + \frac{\partial \dot{\mathrm{y}}}{\partial \mathrm{y}} + \frac{\partial \dot{\mathrm{z}}}{\partial \mathrm{z}} = -2 = r \tag{3}$$

with $r = -2$, where r is a negative value. Dynamical system (1) is one dissipative system, and an exponential contraction rate of the system (1) is

$$\frac{\mathrm{dV}}{\mathrm{dt}} = e^{r} = e^{-2} \tag{4}$$

In the chaotic system (1), a volume factor V_0 is seemingly contracted by the flow into a volume factor $V_0 e^{rt} = V_0 e^{-2t}$ in time t. This shows that as t approaches infinity at an exponential rate of r, each volume containing the trajectory of this dynamical system shrinks to zero. Therefore, all this dynamical system orbits are finally confined to a private subset which has zero volume and the asymptotic motion settles onto an attractor of the system (1).

Detailed equilibrium points analyses are performed for the following values of parameter 'a' :

$$a = \tau^{-2} = \frac{1}{\tau^2} = \frac{3-\sqrt{5}}{2}$$

$$a = \tau^{-1} = \frac{1}{\tau} = \frac{-1+\sqrt{5}}{2}$$

$$a = \tau^{0} = 1$$

$$a = \tau^{1} = \frac{1+\sqrt{5}}{2}$$

$$a = \tau^{2} = \frac{3+\sqrt{5}}{2}$$

$$a = -\tau^{-2} = -\frac{1}{\tau^2} = \frac{\sqrt{5}-3}{2}$$

$$a = -\tau^{-1} = -\frac{1}{\tau} = \frac{1-\sqrt{5}}{2}$$

$$a = -\tau^{0} = -1$$

$$a = -\tau^{1} = \frac{-1-\sqrt{5}}{2}$$

$$a = -\tau^{2} = \frac{-3-\sqrt{5}}{2}$$

Table 1: Equlibrium points corresponding to the parameter values of 'a'

PARAMETER 'a'	**EQULIBRIUM POINTS for x, y, z state variables**			
	E1	E2	E3	E4
$\tau^{-2} = \frac{1}{\tau^2} = \frac{3-\sqrt{5}}{2}$	$\frac{1}{\sqrt{\tau}}$ $-\frac{1}{\tau\sqrt{\tau}}$ τ	$-\frac{1}{\sqrt{\tau}}$ $\frac{1}{\tau\sqrt{\tau}}$ τ	$\frac{j}{\tau\sqrt{\tau}}$ $\frac{j}{\sqrt{\tau}}$ $-\frac{1}{\tau}$	$\frac{-j}{\tau\sqrt{\tau}}$ $\frac{-j}{\sqrt{\tau}}$ $-\frac{1}{\tau}$
$\tau^{-1} = \frac{1}{\tau} = \frac{-1+\sqrt{5}}{2}$	1 $-\frac{1}{\tau}$ τ	-1 $\frac{1}{\tau}$ τ	$\frac{j}{\tau}$ j $-\frac{1}{\tau}$	$-\frac{j}{\tau}$ $-j$ $-\frac{1}{\tau}$
$\tau^{0} = 1$	$\sqrt{\tau}$ $-\frac{1}{\sqrt{\tau}}$ τ	$-\sqrt{\tau}$ $\frac{1}{\sqrt{\tau}}$ τ	$\frac{j}{\sqrt{\tau}}$ $j\sqrt{\tau}$ $-\frac{1}{\tau}$	$-\frac{j}{\sqrt{\tau}}$ $-j\sqrt{\tau}$ $-\frac{1}{\tau}$
$\tau^{1} = \frac{1+\sqrt{5}}{2}$	τ -1 τ	$-\tau$ 1 τ	j $j\tau$ $-\frac{1}{\tau}$	$-j$ $-j\tau$ $-\frac{1}{\tau}$
$\tau^{2} = \frac{3+\sqrt{5}}{2}$	$\tau\sqrt{\tau}$ $-\sqrt{\tau}$ τ	$-\tau\sqrt{\tau}$ $\sqrt{\tau}$ τ	$j\sqrt{\tau}$ $j\tau\sqrt{\tau}$ $-\frac{1}{\tau}$	$-j\sqrt{\tau}$ $-j\tau\sqrt{\tau}$ $-\frac{1}{\tau}$
$-\tau^{-2} = -\frac{1}{\tau^2} = \frac{\sqrt{5}-3}{2}$	$\frac{j}{\sqrt{\tau}}$ $-\frac{j}{\tau\sqrt{\tau}}$ τ	$-\frac{j}{\sqrt{\tau}}$ $\frac{j}{\tau\sqrt{\tau}}$ τ	$\frac{1}{\tau\sqrt{\tau}}$ $\frac{1}{\sqrt{\tau}}$ $-\frac{1}{\tau}$	$-\frac{1}{\tau\sqrt{\tau}}$ $-\frac{1}{\sqrt{\tau}}$ $-\frac{1}{\tau}$
$-\tau^{-1} = -\frac{1}{\tau} = \frac{1-\sqrt{5}}{2}$	j $-\frac{j}{\tau}$ τ	$-j$ $\frac{j}{\tau}$ τ	$\frac{1}{\tau}$ 1 $-\frac{1}{\tau}$	$-\frac{1}{\tau}$ -1 $-\frac{1}{\tau}$
$-\tau^{0} = -1$	$j\sqrt{\tau}$ $-j\frac{1}{\sqrt{\tau}}$ τ	$-j\sqrt{\tau}$ $j\frac{1}{\sqrt{\tau}}$ τ	$\frac{1}{\sqrt{\tau}}$ $\sqrt{\tau}$ $-\frac{1}{\tau}$	$-\frac{1}{\sqrt{\tau}}$ $-\sqrt{\tau}$ $-\frac{1}{\tau}$
$-\tau^{1} = \frac{-1-\sqrt{5}}{2}$	$j\tau$ $-j$ τ	$-j\tau$ j τ	1 τ $-\frac{1}{\tau}$	-1 $-\tau$ $-\frac{1}{\tau}$
$-\tau^{2} = \frac{-3-\sqrt{5}}{2}$	$j\tau\sqrt{\tau}$ $-j\sqrt{\tau}$ τ	$-j\tau\sqrt{\tau}$ $j\sqrt{\tau}$ τ	$\sqrt{\tau}$ $\tau\sqrt{\tau}$ $-\frac{1}{\tau}$	$-\sqrt{\tau}$ $-\tau\sqrt{\tau}$ $-\frac{1}{\tau}$

Equilibrium points of x, y, z state variables corresponding to the parameter values of 'a' are shown in Table 1. System has four equilibrium points. Two of them are real and two of them are imaginary in all situations in Table 1. It is clearly seen in Table 1 that, the new system exactly have golden proportion equilibrium points for all parameter values. It is interesting that amplitudes of real and imaginary equilibrium points are mutually displaced, when sign of 'a' changed positive to negative. The celebrated Golden Proportion $\tau = \frac{1+\sqrt{5}}{2}$ is often seen in nature and examined in modern physical research in the last years [18, 19, 51].

2.3. Lyapunov exponents spectrum and fractional dimension

Lyapunov exponent spectrum of new chaotic system shown in Figure 2 is symmetrical relative to a = 0. The spectrum shows the parameter a is varying in the range of -5 and +5 with 0.01 steps. The system is in chaos when lyapunov exponents are positive, zero and negative $(+, 0, -)$ in some regions like in Figure 2.

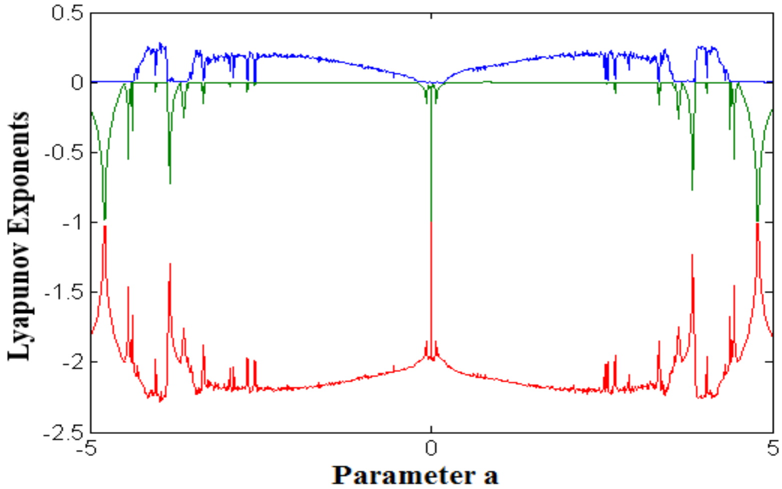

Figure 2: Lyapunov exponents spectrum of new system when a is varying between -5 and +5.

For the negative values of parameter a, system first enters chaos about $a = -4.4$. Between $a = -4.4$ and $a = -2.5$ the system enters to and exits from chaotic zone several times. After $a = -2.5$ the system is always chaotic until $a = -0.25$. For the positive values of parameter a, system first enters chaos about $a = 0.25$. Between $a = 0.25$ and $a = 2.5$ system is always chaotic. And the system exits from chaotic zone about $a = 4.4$. Lyapunov dimension of the system is calculated from Lyapunov exponent spectrum graph by the formula; (for $a = 0.5, L1 = 0.09, L2 = 0, L3 = -2.05$)

$$D_L = j + \frac{1}{|L_j + 1|}\sum_{i=1}^{j}(L_i) = 2 + \frac{L_1 + L_2}{|L_3|} = 2.043902$$

Rounding 2.043902 up to 3 shows that the system is three-dimensional continuous time chaotic system and Lyapunov dimensions of the system are fractional.

2.4. Bifurcation analysis

Figure 3 shows bifurcation diagram of the system when parameter a is varying between -5 and +5. It is clearly seen from the Figure 3 that chaotic zone limits of parameter a are consistent with the Lyapunov exponent spectrum shown in Figure 2. The system enters to and exits from chaotic zones several times.

In the Figure 3 multiple lines or dots for the same value of parameter a show that system is chaotic for this value. For the values between $a = -4.5$ and $a = 4.5$ the system is mostly chaotic. The system is not chaotic out of this zone.

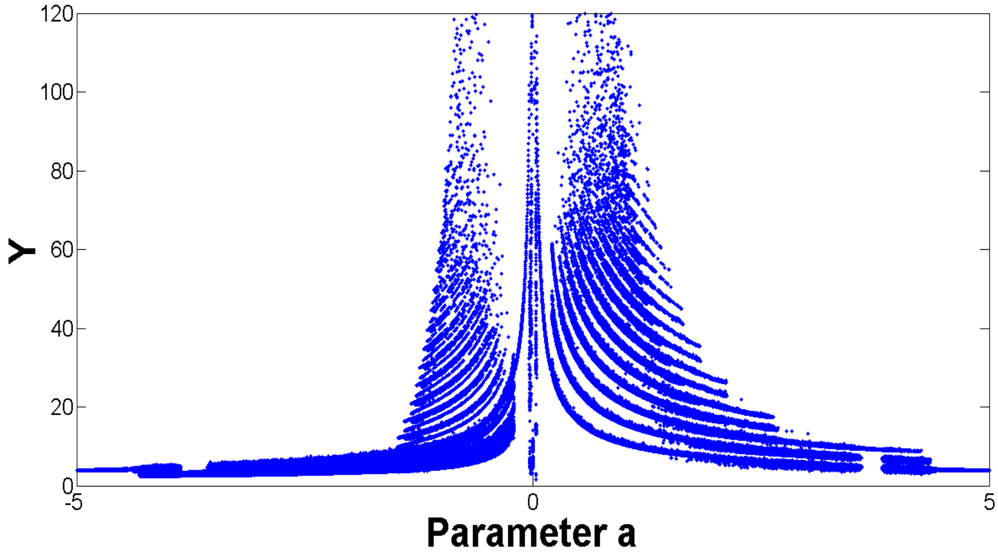

Figure 3: Bifurcation diagram when a is varying between -5 and +5.

3. Hidden amplitude control properties and coexisting attractors

To achieve adequate amplitude control, we introduce a parameter in a quadratic coefficient to achieve partial amplitude control of the chaotic system. Hidden amplitude control properties of the system is achieved by adding a coefficient b in the quadratic term xy in the third dimension of system (1).

$$\begin{cases} \dot{x} = -x - yz, \\ \dot{y} = x - y - xz, \\ \dot{z} = bxy + a, \end{cases} \tag{5}$$

If we take $b \to kb$, $x \to x/\sqrt{k}$, $y \to y/\sqrt{k}$, $z \to z$,

in Eq. (5), the resulting system is identical to system (1), which means that parameter b can control the amplitude of variables x and y according to $1/\sqrt{k}$, while leaving the variable z unchanged. To show this interesting feature, b parameter values were taken as $b = 1, b = 0.25$ and $b = 4$, and also their phase portraits were achieved and showed in Figures 4-6 respectively. As can be seen in Figures 4-6, amplitudes of variables x and y are multiplied by 2, and then divided by 2, according to their corresponding amplitude control factors $1/\sqrt{0.25}$ and $1/\sqrt{4}$. In simulations, initial conditions of $x(0), y(0)$ and $z(0)$ variables are taken as $1, 0$, and 0 respectively.

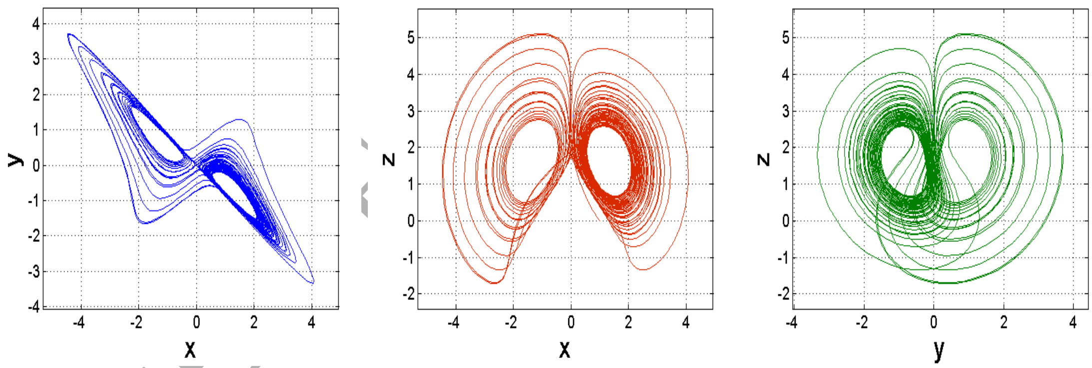

(a) (b) (c)

Figure 4: Phase portraits of the system when b=1, a)$x - y$ plane, b)$x - z$ plane, c)$y - z$ plane

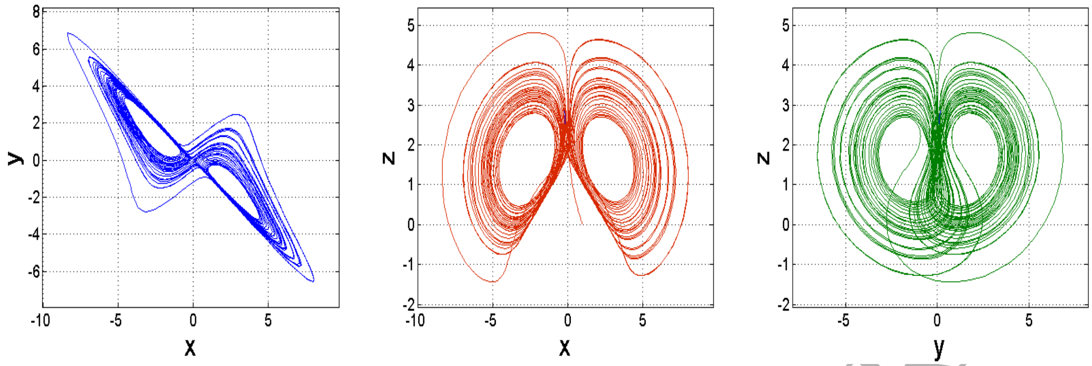

(a) (b) (c)

Figure 5: Phase portraits of the system when $b = 0.25$. Amplitudes of variables x and y are multiplied by 2, according to amplitude control factors $1/\sqrt{0.25}$, while leaving the variable z unchanged, a)$x - y$ plane, b)$x - z$ plane, c)$y - z$ plane

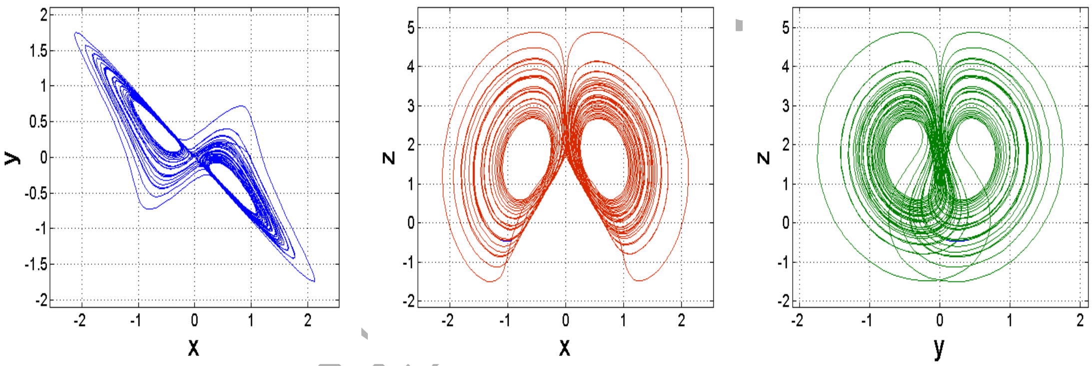

(a) (b) (c)

Figure 6: Phase portraits of the system when b=4. Amplitudes of variables x and y are divided by 2, according to amplitude control factors $1/\sqrt{4}$, while leaving the variable z unchanged, a)$x - y$ plane, b)$x - z$ plane, c)$y - z$ plane

4. The electronic circuit application of the new 3D chaotic system

Electronic circuit of the 3D chaotic system (2) is implemented. The parameters values are adjusted to $a = 1$ for electronic circuit application. The time series of the new chaotic system are seen in Figure 7.

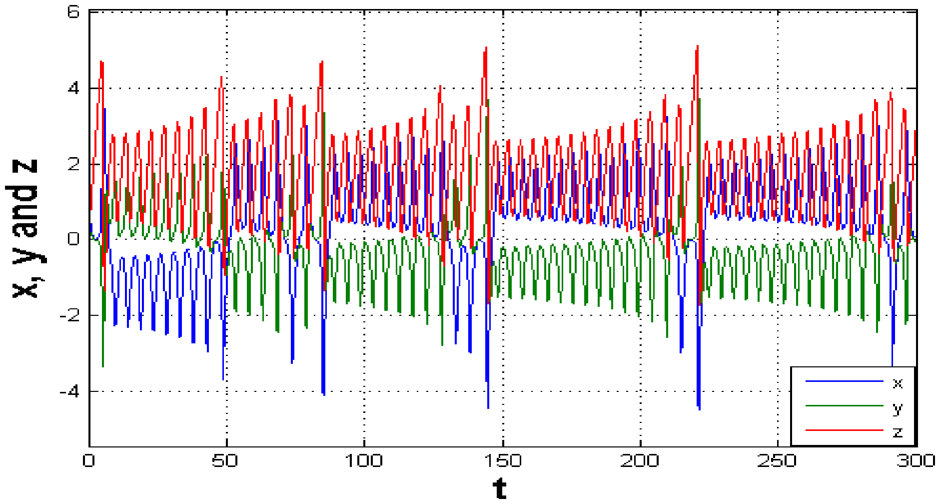

Figure 7: The time series signals of the new chaotic system for x, y and z (ms)

The signal values must be in the linear range of operational amplifiers for electronic design. All the chaotic signal values are in the interval of $(-15, 15)$ as seen in Figure 7. Therefore the circuit can be realized using ordinary electronic components and signal values dont need to be scaled for real-time application. We can directly implement the electronic circuit without scaling.

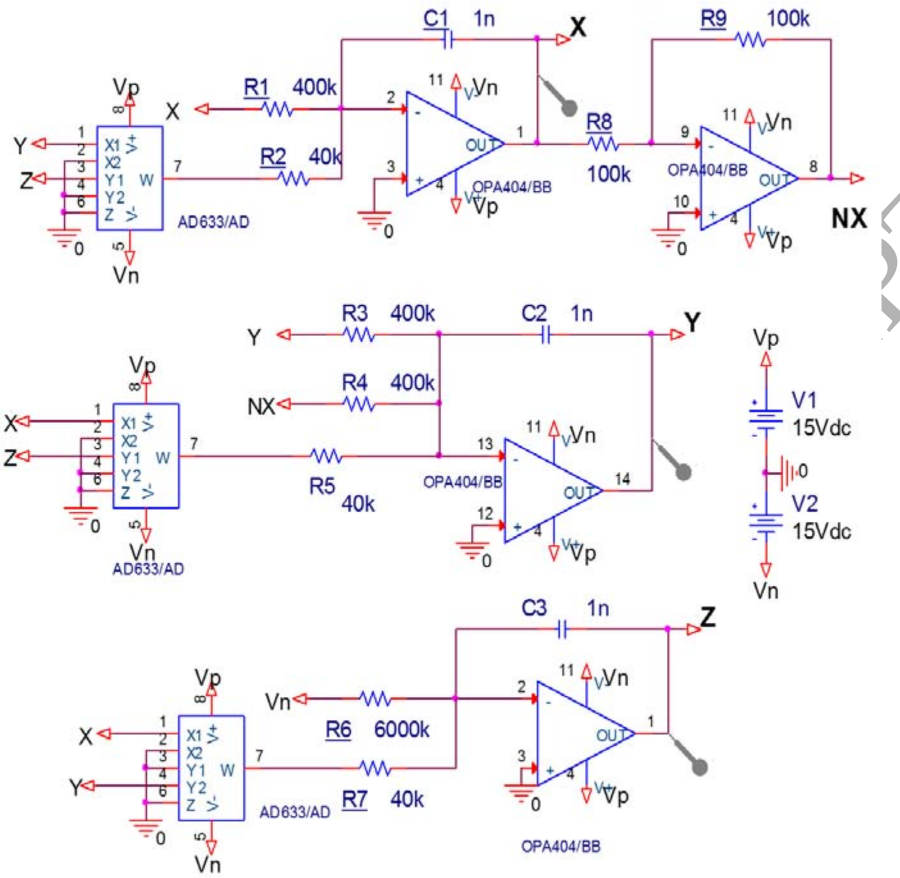

Figure 8: The circuit schematic diagram of the new chaotic system

To obtain the nonlinear system in Eq. (1), state variables are provided as in Eq. (6). The values of electronic component are calculated by using Eq. (6). An electronic circuit is designed as shown in Figure 8 for new chaotic system. Select $C1 = C2 = C3 = 1nF$, $R1 = R3 = R4 = 100k$, $R2 = R5 = R7 = 40k$, $R6 = 6000k$ and $R8 = R9 = 100k$. Corresponding phase portraits in ORCAD - PSpice and on the oscilloscope are shown in Figure 9 and Figure 10. The circuit is powered by $+15V$ and $-15V$ DC supply. Real electronic circuit implementation of the new chaotic system on a test board is shown in Figure 11.

$$\begin{cases} \dot{x} = -\frac{1}{R_1C_1}x - \frac{1}{R_2C_1}yz, \\ \dot{y} = \frac{1}{R_4C_2}x - \frac{1}{R_3C_2}y, -\frac{1}{R_5C_2}xz, \\ \dot{z} = \frac{1}{R_7C_3}xy + \frac{1}{R_6C_3} \end{cases} \quad (6)$$

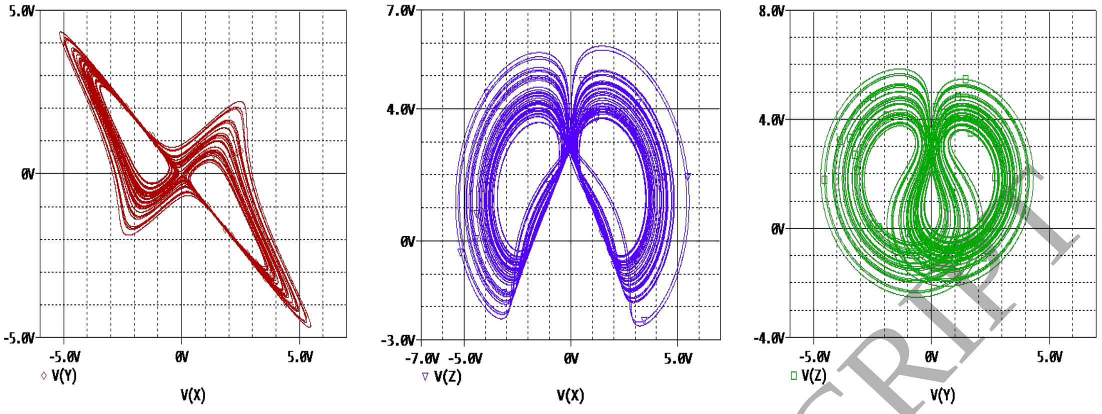

(a) (b) (c)

Figure 9: The phase portraits of the new chaotic system in ORCAD-PSpice, a)$x-y$ plane, b)$x-z$ plane, c)$y-z$ plane

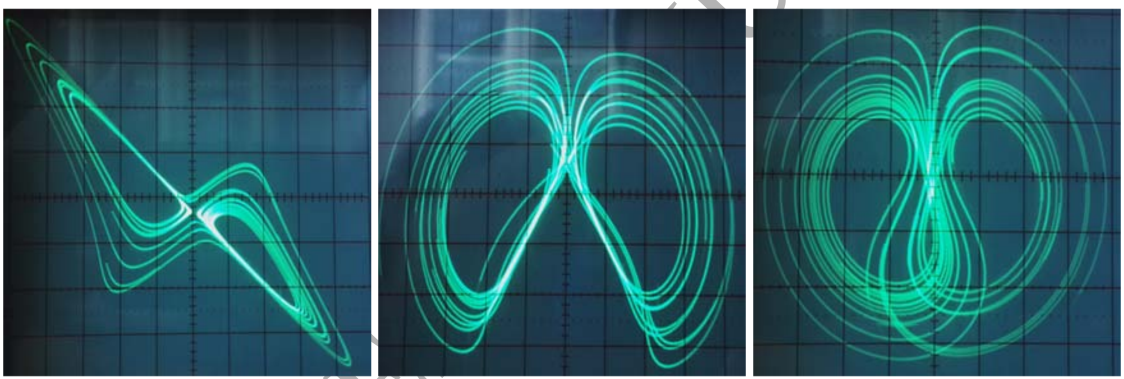

(a) (b) (c)

Figure 10: The phase portraits of the new chaotic system on the oscilloscope, a)$x-y$ plane, b)$x-z$ plane, c)$y-z$ plane (Volt/Div=2V, for all planes)

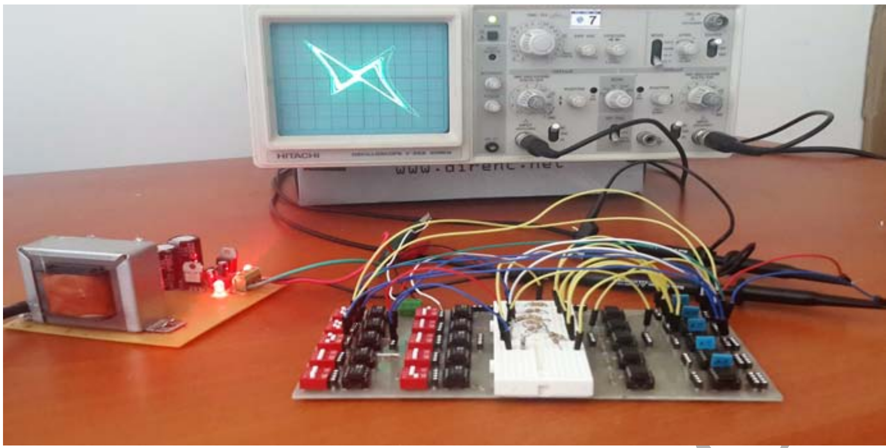

Figure 11: The experimental circuit of the new chaotic system

By using R6= 6k ohm, parameter a=1 is chosen for circuit implementation. Small changes on R6 resistance value or any external noisy signal may cause some small changes on the parameter a value. However the system is still chaotic as it can be seen on Lyapunov Exponents Spectrum in Figure 2 where the system is always chaotic for all the values of the parameter a between 0.25 and 2.5. On the other side, the system has hidden amplitude control property as explained in section 3 which enables to get required chaotic signal with any desired amplitude level by setting the resistance value of R7 easily using an adjustable resistor.

Thanks to large chaotic range of the parameter a and adjustable amplitude control property, the chaotic system and its electronic circuit implementation have robust chaotic dynamics.

5. Microcomputer-based random number generator (RNG)

Nowadays, some random number generators are implemented by using high-cost hardware like FPGA and computers [11, 52, 53]. In this section we designed a low-cost random number generator by using 64-bit quad-core ARM Cortex-A53 microprocessor based "Raspberry Pi 3" microcomputer board which has several external interface ports. Design steps of random number generator, implemented in Raspberry Pi 3 using Python programming language, are shown in Figure 12. At first step, parameters and initial values of the chaotic system are entered. Then by using RK4 method, continuous time chaotic system is solved and converted to discrete system. After discretization, 3 different series of float numbers are obtained. Each of x, y and z series of numbers or their different combinations can be used to generate random numbers. In this study, only z series numbers are preferred. Then z numbers in float format are converted to 32 bit binary. LSB 4 bits from each 32-bit number are extracted to compose random bit series.

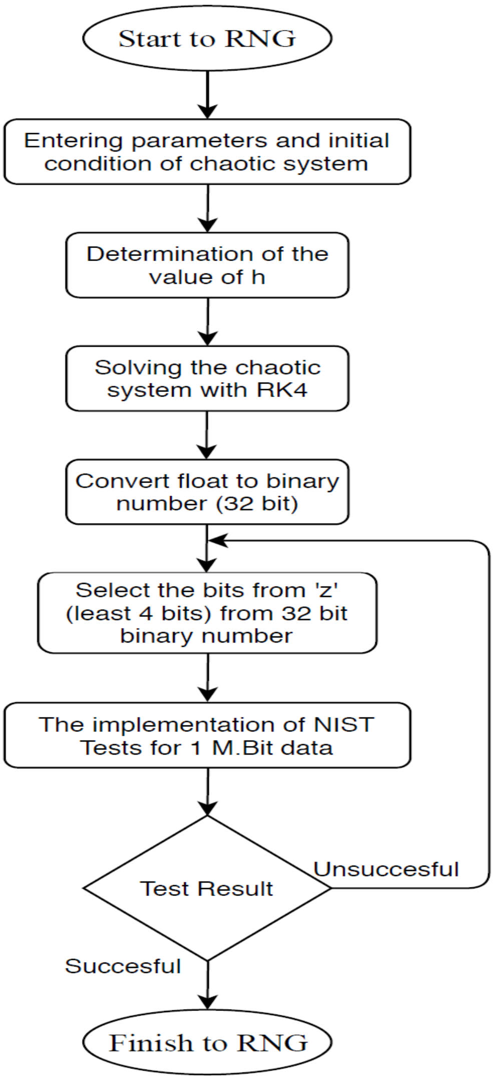

Figure 12: Random number generator design steps

In order to test and verify the randomness of generated bit series, NIST-800-22 test suite, which is the most reliable and internationally proved test suite currently available, is used. For NIST-800-22 tests at least 1 Mbit series of bits are required as input. At each test step, resulted $Pvalue$ shall be greater than 0.001 to pass the test. The generated bit series extracted from LSB 4 bits of z output of the chaotic system has passed all tests successfully. Test results are given in Table 2.

Table 2: NIST-800-22 test results for z output

Statistical Tests	**P-value (Z_4bit)**	**Result**
Frequency (Monobit) Test	0.5445	Successful
Block-Frequency Test	0.4404	Successful
Cumulative-Sums Test	0.8358	Successful
Runs Test	0.0514	Successful
Longest-Run Test	0.1896	Successful
Binary Matrix Rank Test	0.3705	Successful
Discrete Fourier Transform Test	0.2438	Successful
Non-Overlapping Templates Test	0.0742	Successful
Overlapping Templates Test	0.6543	Successful
Maurer's Universal Statistical Test	0.4279	Successful
Approximate Entropy Test	0.7380	Successful
Random-Excursions Test (x = -4)	0.2700	Successful
Random-Excursions Variant Test (x = 9)	0.5700	Successful
Serial Test-1	0.3697	Successful
Serial Test-2	0.8689	Successful
Linear-Complexity Test	0.7117	Successful

The random bit series from z output of the chaotic system that passed all NIST-800-22 tests is produced by Raspberry Pi 3 microcomputer GPIO (General purpose input/output) pin 38 shown in Figure 13.

Figure 13: 'z' output of the new chaotic system on "Raspberry Pi 3" microcomputer board

In Figure 14 several views of random bit series, produced from z output, on oscilloscope screen are given. The generated random bit series can be useful in real-world applications where random numbers needed. Main advantages of the random number generator are low-cost design and mobility.

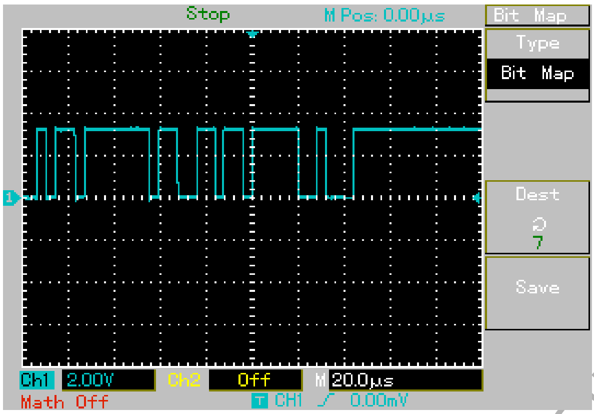

(a)

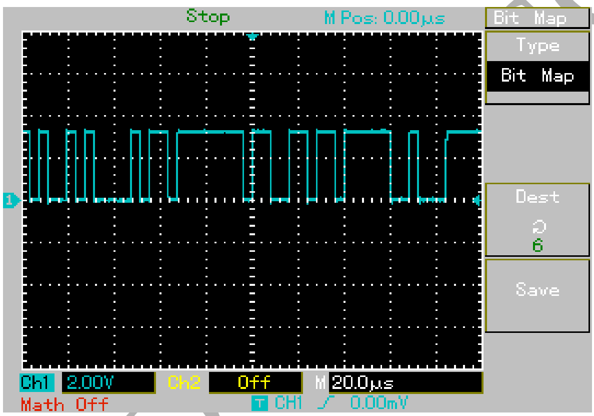

(b)

Figure 14: Oscilloscope screens of the random bit series produced from 'z' output(250 KHz), a) Sample screen output 1, b) Sample screen output 2.

6. Conclusions

In this paper, we proposed a strange novel three-dimensional chaotic system with golden proportion equilibria. One notable feature of chaotic system is that it has equilibrium points which are fully golden proportion values. In addition, the strange chaotic system has hidden amplitude control properties presented in section 3.After dynamical analyses, the chaotic system is implemented as an electronic circuit. A microcomputer-based RNG is also designed using this chaotic attractor. RNG results are tested and successfully passed the universal NIST-800-22 tests.

Acknowledgments

This work is supported by the Scientific and the Research Council of Turkey (TUBITAK) under Grant No. 117E284 and Sakarya University Scientific Research Projects Unit under Grants 2017-09-00-010.

References

[1] E. N. Lorenz, Deterministic nonperiodic flow, Journal of the atmospheric sciences 20 (2) (1963) 130–141.

[2] O. E. Rössler, An equation for continuous chaos, Physics Letters A 57 (5) (1976) 397–398.

[3] R. Shaw, Strange attractors, chaotic behavior, and information flow, Zeitschrift für Naturforschung A 36 (1) (1981) 80–112.

[4] J. C. Sprott, Some simple chaotic flows, Physical review E 50 (2) (1994) R647.

[5] J. Sprott, Simplest dissipative chaotic flow, Physics letters A 228 (4-5) (1997) 271–274.

[6] G. Chen, T. Ueta, Yet another chaotic attractor, International Journal of Bifurcation and chaos 9 (07) (1999) 1465–1466.

[7] J. C. Sprott, A new class of chaotic circuit, Physics Letters A 266 (1) (2000) 19–23.

[8] T. Ueta, G. Chen, Bifurcation analysis of chen's equation, International Journal of Bifurcation and Chaos 10 (08) (2000) 1917–1931.

[9] P. Cai, Z. Yuan, Hopf bifurcation and chaos control in a new chaotic system via hybrid control strategy, Chinese Journal of Physics 55 (1) (2017) 64–70.

[10] I. Pehlivan, Y. UYAROĞLU, A new chaotic attractor from general lorenz system family and its electronic experimental implementation, Turkish Journal of Electrical Engineering & Computer Sciences 18 (2) (2010) 171–184.

[11] A. Akgul, I. Moroz, I. Pehlivan, S. Vaidyanathan, A new four-scroll chaotic attractor and its engineering applications, Optik-International Journal for Light and Electron Optics 127 (13) (2016) 5491–5499.

[12] A. Akgul, S. Hussain, I. Pehlivan, A new three-dimensional chaotic system, its dynamical analysis and electronic circuit applications, Optik-International Journal for Light and Electron Optics 127 (18) (2016) 7062–7071.

[13] M. Varan, A. Akgul, Control and synchronisation of a novel seven-dimensional hyperchaotic system with active control, Pramana 90 (4) (2018) 54.

[14] İ. Koyuncu, İ. Şahin, C. Gloster, N. K. Sarıtekin, A neuron library for rapid realization of artificial neural networks on fpga: A case study of rössler chaotic system, Journal of Circuits, Systems and Computers 26 (01) (2017) 1750015.

[15] M. Tuna, C. B. Fidan, Electronic circuit design, implementation and fpga-based realization of a new 3d chaotic system with single equilibrium point, Optik-International Journal for Light and Electron Optics 127 (24) (2016) 11786–11799.

[16] A. Stakhov, Fundamentals of a new kind of mathematics based on the golden section, Chaos, Solitons & Fractals 27 (5) (2006) 1124–1146.

[17] J. Cahn, D. Gratias, B. Mozer, A 6-d structural model for the icosahedral (al, si)-mn quasicrystal, Journal de Physique 49 (7) (1988) 1225–1233.

[18] M. El Naschie, On dimensions of cantor set related systems, Chaos, Solitons & Fractals 3 (6) (1993) 675–685.

[19] M. El Naschie, Quantum mechanics and the possibility of a cantorian space-time, Chaos, Solitons & Fractals 1 (5) (1991) 485–487.

[20] M. El Naschie, Is quantum space a random cantor set with a golden mean dimension at the core?, Chaos, Solitons & Fractals 4 (2) (1994) 177–179.

[21] M. El Naschie, Fredholm operators and the wave-particle duality in cantorian space, Chaos, Solitons & Fractals 9 (6) (1998) 975–978.

[22] M. El Naschie, Complex vacuum fluctuation as a chaotic limit set of any kleinian group transformation and the mass spectrum of high energy particle physics via spontaneous self-organization, Chaos, Solitons & Fractals 17 (4) (2003) 631–638.

[23] M. El Naschie, Topological defects in the symplictic vacuum, anomalous positron production and the gravitational instanton, International Journal of Modern Physics E 13 (04) (2004) 835–849.

[24] M. El Naschie, Experimental and theoretical arguments for the number and the mass of the higgs particles, Chaos, Solitons & Fractals 23 (4) (2005) 1091–1098.

[25] M. El Naschie, Anomaly cancellation and the mass spectrum of ε (), Chaos, Solitons & Fractals 23 (3) (2005) 1087–1090.

[26] S. Boccaletti, J. Kurths, G. Osipov, D. Valladares, C. Zhou, The synchronization of chaotic systems, Physics reports 366 (1) (2002) 1–101.

[27] J. Lü, X. Yu, G. Chen, Chaos synchronization of general complex dynamical networks, Physica A: Statistical Mechanics and its Applications 334 (1) (2004) 281–302.

[28] L. Chun-Biao, C. Su, Z. Huan-Qiang, Circuit implementation and synchronization of an improved system with invariable lyapunov exponent spectrum.

[29] C. Li, H. Wang, An extension system with constant lyapunov exponent spectrum and its evolvement study, Acta Phys. Sin 58 (11) (2009) 7514–7524.

[30] C. Li, J. Wang, W. Hu, Absolute term introduced to rebuild the chaotic attractor with constant lyapunov exponent spectrum, Nonlinear Dynamics 68 (4) (2012) 575–587.

[31] C. Li, J. Sprott, Amplitude control approach for chaotic signals, Nonlinear Dynamics 73 (3) (2013) 1335–1341.

[32] C. Li, J. C. Sprott, Z. Yuan, H. Li, Constructing chaotic systems with total amplitude control, International Journal of Bifurcation and Chaos 25 (10) (2015) 1530025.

[33] W. Hu, A. Akgul, C. Li, T. Zheng, P. Li, A switchable chaotic oscillator with two amplitude–frequency controllers, Journal of Circuits, Systems and Computers (2017) 1750158.

[34] C. Li, I. Pehlivan, J. C. Sprott, Amplitude-phase control of a novel chaotic attractor, Turkish Journal of Electrical Engineering and Computer Sciences 24 (2016) 1–11.

[35] A. Akgul, H. Calgan, I. Koyuncu, I. Pehlivan, A. Istanbullu, Chaos-based engineering applications with a 3d chaotic system without equilibrium points, Nonlinear Dynamics 84 (2) (2016) 481–495.

[36] H. Nejati, A. Beirami, W. H. Ali, Discrete-time chaotic-map truly random number generators: design, implementation, and variability analysis of the zigzag map, Analog Integrated Circuits and Signal Processing 73 (1) (2012) 363–374.

[37] L. Zhao, X. Liao, D. Xiao, T. Xiang, Q. Zhou, S. Duan, True random number generation from mobile telephone photo based on chaotic cryptography, Chaos, Solitons & Fractals 42 (3) (2009) 1692–1699.

[38] C. Li, I. Pehlivan, J. C. Sprott, A. Akgul, A novel four-wing strange attractor born in bistability, IEICE Electronics Express 12 (4) (2015) 20141116–20141116.

[39] K. Vishal, S. K. Agrawal, On the dynamics, existence of chaos, control and synchronization of a novel complex chaotic system, Chinese Journal of Physics 55 (2) (2017) 519–532.

[40] P. Gholamin, A. R. Sheikhani, A new three-dimensional chaotic system: dynamical properties and simulation, Chinese Journal of Physics 55 (4) (2017) 1300–1309.

[41] P. Bratley, B. L. Fox, L. E. Schrage, A guide to simulation, Springer Science & Business Media, 2011.

[42] C. B. FİDAN, M. TUNA, Kaotik sistemler ve fpga tabanlı kaotik osilatörlerin gerçek rasgele sayı üretimindeki (grsü) önemi üzerine bir araştırma, Gazi Üniversitesi Mühendislik-Mimarlık Fakültesi Dergisi 2018 (2018).

[43] Ç. K. Koç, About cryptographic engineering, in: Cryptographic engineering, Springer, 2009, pp. 1–4.

[44] T. Tuncer, E. Avaroglu, M. Türk, A. B. Ozer, Implementation of non-periodic sampling true random number generator on fpga, Informacije MIDEM 44 (4) (2015) 296–302.

[45] I. Vasyltsov, E. Hambardzumyan, Y.-S. Kim, B. Karpinskyy, Fast digital trng based on metastable ring oscillator, in: International Workshop on Cryptographic Hardware and Embedded Systems, Springer, 2008, pp. 164–180.

[46] M. E. Yalcin, J. A. Suykens, J. Vandewalle, True random bit generation from a double-scroll attractor, IEEE Transactions on Circuits and Systems I: Regular Papers 51 (7) (2004) 1395–1404.

[47] Y. Hu, X. Liao, K.-w. Wong, Q. Zhou, A true random number generator based on mouse movement and chaotic cryptography, Chaos, Solitons & Fractals 40 (5) (2009) 2286–2293.

[48] F. Pareschi, G. Setti, R. Rovatti, A fast chaos-based true random number generator for cryptographic applications, in: Solid-State Circuits Conference, 2006. ESSCIRC 2006. Proceedings of the 32nd European, IEEE, 2006, pp. 130–133.

[49] S. Ergun, S. Ozoguz, A chaos-modulated dual oscillator-based truly random number generator, in: Circuits and Systems, 2007. ISCAS 2007. IEEE International Symposium on, IEEE, 2007, pp. 2482–2485.

[50] A. Beirami, H. Nejati, Y. Massoud, A performance metric for discrete-time chaos-based truly random number generators, in: Circuits and Systems, 2008. MWSCAS 2008. 51st Midwest Symposium on, IEEE, 2008, pp. 133–136.

[51] A. Maiboroda, Finding the golden section in fundamental relations of physical magnitudes, in: Proceedings of the international conference Problems of harmony, symmetry and the golden section in nature, science and art, Vol. 15, 2003, pp. 87–94.

[52] Ü. Çavuşoğlu, A. Akgül, S. Kaçar, İ. Pehlivan, A. Zengin, A novel chaos-based encryption algorithm over tcp data packet for secure communication, Security and Communication Networks.

[53] D. Schellekens, B. Preneel, I. Verbauwhede, Fpga vendor agnostic true random number generator, in: Field Programmable Logic and Applications, 2006. FPL'06. International Conference on, IEEE, 2006, pp. 1–6.